

## Coherent Scattering of a Multiphoton Quantum Superposition by a Mirror BEC

Francesco De Martini,<sup>1,2</sup> Fabio Sciarrino,<sup>2</sup> Chiara Vitelli,<sup>1</sup> and Francesco S. Cataliotti<sup>3</sup>

<sup>1</sup>*Dipartimento di Fisica, Università di Roma “La Sapienza,” Piazzale Aldo Moro 2, I-00185 Roma, Italy*

<sup>2</sup>*Accademia Nazionale dei Lincei, Via della Lungara 10, I-00165 Roma, Italy*

<sup>3</sup>*Dipartimento di Energetica and LENS, Università di Firenze, via N. Carrara 1, I-50019 Sesto F.no (FI), Italy*

(Received 28 February 2009; published 3 February 2010)

We present the proposition of an experiment in which the multiphoton quantum superposition consisting of  $\mathcal{N} \approx 10^5$  particles generated by a quantum-injected optical parametric amplifier, seeded by a single-photon belonging to an Einstein-Podolsky-Rosen entangled pair, is made to interact with a mirror-Bose-Einstein condensate (BEC) shaped as a Bragg interference structure. The overall process will realize a macroscopic quantum superposition involving a microscopic single-photon state of polarization entangled with the coherent macroscopic transfer of momentum to the BEC structure, acting in spacelike separated distant places.

DOI: 10.1103/PhysRevLett.104.050403

PACS numbers: 03.65.Ud, 03.67.-a, 03.75.Gg

In recent years, a great deal of interest has been focused on the ambitious problem of creating a macroscopic quantum superposition (MQS) of a massive object by an entangled optomechanical interaction of a tiny mirror with a single photon within a Michelson interferometer [1–5], then realizing a well-known 1935 argument by Erwin Schrödinger [6]. The present work is aimed at a similar scope but is not concerned with interferometers nor with solid mirrors. It rather exploits the process of nonresonant scattering by a properly shaped Bose-Einstein condensate (BEC) [7] of an externally generated multiparticle quantum photon state, a “macrostate”  $|\Phi\rangle$ , in order to create a joint atom-photon macrostate entangled by momentum conservation. Light scattering from BEC structures has been used so far to enhance their nonlinear macroscopic properties in superradiance experiments [8] to show the possibility of matter-wave amplification [9] and nonlinear wave mixing [10]. In the present work, we intend to discuss the linear *coherent scattering*, i.e., the *reflection* by a multilayered BEC of a large assembly of nearly monochromatic photons generated by a high-gain “quantum-injected” optical parametric amplifier (QI-OPA) in a Einstein-Podolsky-Rosen (EPR) configuration [11,12]. Very recently, it was demonstrated experimentally that the optical macrostate  $|\Phi\rangle$  generated by the QI-OPA can indeed be entangled with, i.e., nonseparable from, a far apart single-photon state belonging to the injected EPR pair [13], thus resulting highly resilient to the decoherence due to losses [14]. By the present work, this condition will be extended to the mechanical motion of an atomic assembly by making the photonic macrostate  $|\Phi\rangle$  to exchange linear momentum with a high reflectivity BEC optical mirror, here referred to as a “mirror BEC” (mBEC). This can be a novel and viable alternative to the realization of an entangled MQS of a massive object.

The layout of the experiment, Fig. 1, shows an EPR optical parametric amplifier, provided by Crystal 1, of a polarization entangled ( $\pi$ -entangled) pair of photons

launched towards two distant measurement stations, here referred to as *Alice* (*A*) and *Bob* (*B*) [13,15]. One of the EPR photons emitted towards the Bob’s site is injected into the QI-OPA which generates a corresponding macrostate  $|\Phi\rangle$ . The device operates in the collinear regime and amplifies with a large “gain” any injected single photon in a quantum superposition, i.e., a *qubit*  $|\varphi\rangle_{k_1}$ , into a large number of photons,  $\mathcal{N} \approx 10^5$ , associated with a corresponding macroqubit  $|\Phi^\varphi\rangle_{k_1}$ . These macrostates then drive the mechanical motion of the mBEC. Since these states are found to be entangled with the far apart single-photon emitted over the mode  $\mathbf{k}_2$  and detected by Alice, the same entanglement property is then transferred to the position macrostate of the optically driven mBEC [Fig. 1(b)]. The optical part of the apparatus is the working QI-OPA device recently reported by [13,15] to which the reader is referred.

*Micro-macro entangled light.*—As shown in Fig. 1, the main uv beam is split in two beams and excites two nonlinear (NL) crystals cut for type II phase-matching. Crystal 1 is the spontaneous parametric down-conversion source of entangled photon couples of wavelength (wl)  $\lambda' = 2\lambda'_p$ , emitted over the modes  $\mathbf{k}_i$  ( $i = 1', 2$ ) in the entangled *singlet* state  $|\Psi^-\rangle_{k_1',k_2} = 2^{-1/2}(|H\rangle_{k_1'}|V\rangle_{k_2} - |V\rangle_{k_1'}|H\rangle_{k_2})$ , where  $H(V)$  labels the single-photon state horizontally (vertically) polarized. The photon associated with the mode  $\mathbf{k}_2$  (the *trigger* mode) is coupled to a single mode (SM) fiber and filtered by a set of  $\pi$ -analyzing optical devices, namely, a Babinet compensator (B), a  $\lambda'/2 + \lambda'/4$  wave plate set, a polarizing beam splitter (PBS), and an interference filter (IF) with a transmission linewidth  $\Delta\lambda'$ . At last, the *trigger* photon excites, at the Alice’s site, the single-photon detector  $D_2^A$  delivering the *trigger* signal adopted to establish the overall quantum correlations. By a dichroic mirror (DM), the single photon created over the mode  $\mathbf{k}'_1$  is made to merge into the mode  $\mathbf{k}_1$  together with the uv beam associated with mode  $\mathbf{k}'_p$  and then injected into the NL Crystal 2 where it stimulates the emission of many photon pairs over the two polarization

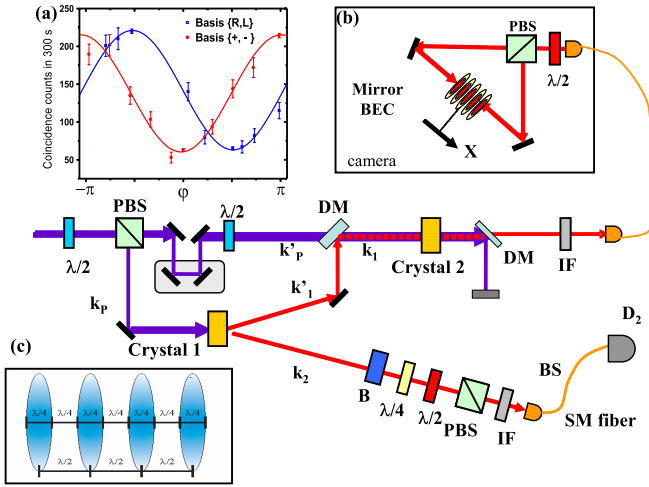


FIG. 1 (color online). Layout of the QI-OPA + M-BEC experimental apparatus. The upper left (a) inset shows the interference patterns detected at the output of the PBS shown in the (b) inset for two different measurement bases  $\{+, -\}$  and  $\{L, R\}$ . Alternating slabs of condensate and vacuum are shown in the lower left (c) inset. A more detailed account of inset (b) is given in Fig. 3.

output modes associated with the spatial mode  $\mathbf{k}_1$ . The injected qubit is prepared in the state  $|\varphi\rangle_{k_1} = 2^{-1/2}(|H\rangle_{k_1} + e^{i\varphi}|V\rangle_{k_1})$  by measuring the photon on mode  $\mathbf{k}_2$  in an appropriate polarization basis.

When a single-photon qubit  $|\pm\rangle = 2^{-1/2}(|H\rangle \pm |V\rangle)$  is injected on mode  $\mathbf{k}_1$ , the amplified output state is expressed as  $|\Phi^\pm\rangle = \sum_{i,j=0}^{\infty} \gamma_{ij} (2i+1)\pm |2j\rangle_{\mp}$  and  $\gamma_{ij} \equiv \sqrt{(1+2i)!(2j)!(i!j!)^{-1}} C^{-2} (-\frac{\Gamma}{2})^i \frac{\Gamma^j}{2}$ ,  $C \equiv \cosh g$ ,  $\Gamma \equiv \tanh g$ , being  $g = \chi t$  the NL gain. There,  $|p\rangle_{+}|q\rangle_{-}$  stands for a state with  $p$  photons with polarization  $\vec{\pi}_{+}$  and  $q$  photons with  $\vec{\pi}_{-}$ . The macrostates  $|\Phi^\pm\rangle$  are orthonormal, i.e.,  $\langle i|\Phi^j\rangle = \delta_{ij}$ . The overall entangled  $|\Sigma\rangle_{k_1, k_2} = 2^{-1/2}(|\Phi^+\rangle_{k_1}|+\rangle_{k_2} - |\Phi^-\rangle_{k_1}|-\rangle_{k_2})$  keeps its *singlet* character in the multiparticle regime between two distant objects: the *microscopic*, i.e., single particle system expressed by the *trigger* state (mode  $\mathbf{k}_2$ ) and the *macroscopic* multiparticle system ( $\mathbf{k}_1$ ) [16]. At the output of Crystal 2 the beam with wvl  $\lambda'$  is spatially separated by the pump uv beam by a DM and an IF with bandwidth 0.75 nm and finally coupled to a single mode fiber. Two counteracting optical beams associated with the macrostates  $|\Phi^\pm\rangle$  for a total of  $\mathcal{N} \approx 3\bar{m} \approx 1.2 \times 10^5$  are spatially separated by a PBS and focused on the opposed sides of a cigar-shaped mBEC.

Let us analyze the output field over the polarization modes  $\vec{\pi}_{\pm}$ , i.e., by adopting the measurement basis  $\{+, -\}$  realized by qubit  $|\varphi\rangle$ . The ensemble average photon number  $N_{\pm}$  emitted over  $\mathbf{k}_1$  depends on the injected phase  $\varphi$ :  $N_{\pm}(\varphi) = \langle \varphi | \Phi | \hat{N}_{\pm}(\varphi) | \Phi \varphi \rangle = \bar{m} + (\bar{m} + \frac{1}{2})(1 \pm \cos \varphi)$  with  $\bar{m} = \sinh^2 g$ , the average value of the number of *squeezed vacuum* photons emitted by OPA in absence of injection [11]. The number difference,  $N(\varphi) = [N_+(\varphi) -$

$N_-(\varphi)] = [(2\bar{m} + 1) \cos \varphi]$ , is expressed by an interference fringe pattern as a function of the phase  $\varphi$  of both the quantum-injected qubit and the EPR correlated trigger qubit [Fig. 1(a)].

*BEC mirror via Bragg reflection.*—Let us now describe the structure of the mBEC and its interaction with light. The dynamics of a BEC loaded in a trap formed by a cylindrically symmetric harmonic potential (either an optical trap or a magnetic trap) with an optical standing wave (SW) aligned along the symmetry axis may be described by the Gross-Pitaevskii equation [17]. If the trap is very elongated, the ground state consists of an array of disks spaced by half the wavelength  $\lambda$  with a longitudinal size  $R_{\parallel} \propto \lambda/s^{-1/4}$  with  $s$  being an adimensional parameter describing the height of the optical lattice in terms of the recoil energy  $E_R = \hbar^2/2m\lambda^2$ . The transverse size  $R_{\perp}$  is dictated by the strength of the magnetic trap and by the number of atoms in the condensate  $N_{\text{at}}$  [18]. The number  $N_D$  of the disks is also fixed by the strength of the magnetic trap in the longitudinal direction and by  $N_{\text{at}}$ . Typical numbers are  $N_D \sim 200$ ,  $N_{\text{at}} \sim 10^6$  with  $R_{\perp} \sim 10 \mu\text{m}$  [19]. By choosing  $s$ , it is then possible to prepare an array of disks with a longitudinal size of  $R_{\parallel} = \frac{\lambda}{4}$  spaced by  $\frac{\lambda}{2}$  [Fig. 1(c)].

Releasing the condensate from the combined trap, the spatial periodic structure is initially preserved as long as the spreading disks do not start to overlap and interfere, and it eventually leads for longer expansion times to a structure that reflects the momentum distribution of the condensate. Both regimes are fundamental to our proposal. If we expose the expanding condensate aligned along the symmetry axis of the harmonic trap to an optical beam with frequency  $\omega - \omega_0 = \Delta$ , largely detuned from the atomic resonance  $\omega_0$ , the dominant scattering mechanism is Rayleigh scattering [8]. The dynamic evolution of the system in this regime is described by the 1D CARL-BEC, i.e., Gross-Pitaevskii, model generalized to include the self-consistent evolution of the scattered radiation amplitude [20–22]:

$$i \frac{\partial \Psi}{\partial t} = -\frac{\hbar^2}{2m} \frac{\partial^2 \Psi}{\partial x^2} + ig \{b^* e^{i(2kx - \delta t)} - \text{c.c.}\} \Psi, \quad (1)$$

$$\frac{da}{dt} = gN \int dx |\Psi|^2 e^{i(2kx - \delta t)} - \kappa a, \quad (2)$$

with  $b = (\epsilon_0 V / 2\hbar \omega_s)^{1/2} E_s$  the dimensionless electric field amplitude of the reflected beam with frequency  $\omega_s$ ,  $g = (\Omega / 2\Delta) (\omega d^2 / 2\hbar \epsilon_0 V)^{1/2}$  the coupling constant, and  $\Omega$  the Rabi frequency modulation of the optical beam;  $d = \hat{\epsilon} \cdot \vec{d}$  is the electric dipole moment of the atom along the polarization direction  $\vec{\epsilon}$  of the laser,  $V$  is the volume of the condensate,  $N$  is the total number of atoms in the condensate, and  $\delta = \omega - \omega_s$  [23]. Let us focus on the amplitude of the reflected beam. We have integrated numerically the Eqs. (1) and (2) with the experimental parameters (given above) of a typical condensate and with the optical parameters for the output of the QI-OPA. As shown by Fig. 2(a),

the normalized amplitude  $a$  of the reflected optical beam drops as the matter-wave grating is deteriorated by the interaction with the light beam. However, during the time duration of a QI-OPA pulse (typically 1 ps), no significant reduction is observed [inset of Fig. 2(a)].

The above result leading to the dependence on  $\omega$  of the mBEC reflectivity has been found consistent with a less sophisticated model of the process based on a classical model for a Bragg mirror. The reflectivity of this one composed by  $2N_D$  alternating layers with refraction index  $n_B \sim (1 + \epsilon)$  is  $R = \left(\frac{n_B^{2N_D} - 1}{n_B^{2N_D} + 1}\right)^2 \sim N_D^2 \epsilon^2$ . For a two-level atom  $\epsilon = \frac{3\pi}{2} \mathcal{M} \frac{\Gamma}{\Delta} \frac{1}{1 + (2\Delta)^2}$ , with  $\mathcal{M} = \lambda^3 \frac{N}{V}$  as the rescaled density,  $\Gamma$  the atomic linewidth, and  $\Delta$  the detuning from resonance. In a rubidium BEC,  $\Gamma \simeq 6$  MHz and typical densities are  $\frac{N}{V} = 10^{14} \text{ cm}^{-3}$ . Combining all of the previous equations and assumptions, we obtain the graph Fig. 2(b). The inset of this figure shows that around the atomic resonance with a bandwidth  $\Delta\nu_a \simeq 8$  GHz, the reflectivity of the patterned BEC is essentially unity [24]. This bandwidth, 3 orders of magnitude larger than in other proposals [25], is instrumental to the proposed experiment sketched in the right inset of Fig. 1. A first estimate of the experimental parameters of the QI-OPA system results in a NL gain  $g = 6\text{--}7$  corresponding to a number of generated photons  $\sim 10^5\text{--}10^6$ . Since the spectral width of the QI-OPA generated beams is  $\Delta\lambda \sim 0.75$  nm, corresponding to a linewidth  $\Delta\nu \sim 350$  GHz, about 3% of the incoming photon beams will be totally reflected by mBEC. This will correspond to a number of active photons  $N'_\pm(\varphi) = (\Delta\nu_a/\Delta\nu) \times N_\pm(\varphi)$  in the range ( $10^3\text{--}10^4$ ). The ratio between the linewidths relative to the absorption (few MHz) and to the reflection process is  $\simeq 0.1\%$ ; hence, the mean number of absorbed photons is about one per pulse, and it follows that the excitation of atoms can be considered negligible during the interaction process. At last, in the future we plan to use a different laser source with a longer pulse duration followed by a periodically poled crystal amplifier. In such a way, it would be possible to obtain a high NL gain value and radiation fields with a bandwidth of  $\sim 10$  GHz.

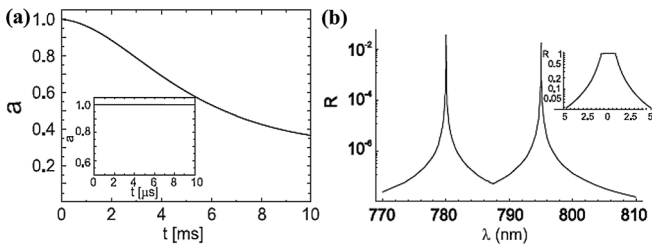


FIG. 2. (a) Normalized amplitude  $a = I(t)/I(0)$ , where  $I(t)$  is the intensity of the reflected beam at time  $t$  after the interaction. In the inset, the normalized amplitude in the first 10  $\mu\text{s}$  is shown. (b) Reflectivity of a patterned BEC as a function of wavelength. The reflectivity around resonance is shown in the inset.

*Measurement of nonlocal correlations.*—In order to observe the recoil effects of the mBEC, the condensate has to be released from the optical lattice that shapes it. This can easily be done by shutting off the laser's light that provides the SW. Typical expansion velocities for a BEC are of the order of 1 nm/ $\mu\text{s}$  which leaves at least 50  $\mu\text{s}$  before the pattern gets significantly spoiled. Let us investigate the different evolution of the BEC motions relative to the impinging field. Consider the case in which the multiphoton field is prepared in the state  $|\Phi^+\rangle$  (or, alternatively,  $|\Phi^-\rangle$ ) on the spatial mode  $\mathbf{k}_1$ . The state can be written as  $|\Phi^+\rangle_1 = |\phi^+\rangle_1 |\xi^-\rangle_1$  ( $|\Phi^-\rangle_1 = |\phi^-\rangle_1 |\xi^+\rangle_1$ ), where  $|\phi^+\rangle$  ( $|\phi^-\rangle$ ) is the wave function contribution with polarization  $\vec{\pi}_+$  ( $\vec{\pi}_-$ ) and  $|\xi^-\rangle$  ( $|\xi^+\rangle$ ) is the contribution with polarization  $\vec{\pi}_-$  ( $\vec{\pi}_+$ ). The number of photons associated to  $|\phi\rangle$  is dominant over the one associated to  $|\xi\rangle$ , as said. The multiphoton state  $|\Phi^+\rangle_1$  ( $|\Phi^-\rangle_1$ ) is sent, through a single mode fiber, toward the BEC condensate. There, a  $\lambda/2$  wave plate and a polarizing beam splitter direct the two polarization components  $\vec{\pi}_+$  and  $\vec{\pi}_-$  over the two spatial modes  $\mathbf{k}_U$  and  $\mathbf{k}_D$ : the macrostate  $|\Phi^+\rangle_1$  ( $|\Phi^-\rangle_1$ ) evolves into  $|\phi^+\rangle_U |\xi^-\rangle_D$  ( $|\xi^+\rangle_U |\phi^-\rangle_D$ ): Fig. 3(a). Then, the two counterpropagating fields are focused on the opposed sides of the cigar-shaped mBEC. Thanks to the large reflectivity of the Bragg structure, an efficient coupling is achieved between the multiphoton fields and the atomic cloud. While the backscattered light pulse changes direction of propagation ( $U \Rightarrow D$ ,  $D \Rightarrow U$ ), the mBEC acquires a momentum kick in the opposite direction to the major photons' contribution  $|\phi^+\rangle_D$  ( $|\phi^-\rangle_D$ ). Hence, after the interaction the overall light-matter state can be written as:  $|\phi^+\rangle_D |\xi^-\rangle_U |\Psi^U\rangle_{\text{bec}}$  ( $|\xi^+\rangle_D |\phi^-\rangle_U |\Psi^D\rangle_{\text{bec}}$ ), where  $|\Psi^U\rangle_{\text{bec}}$  ( $|\Psi^D\rangle_{\text{bec}}$ ) stands for the BEC that recoils in the

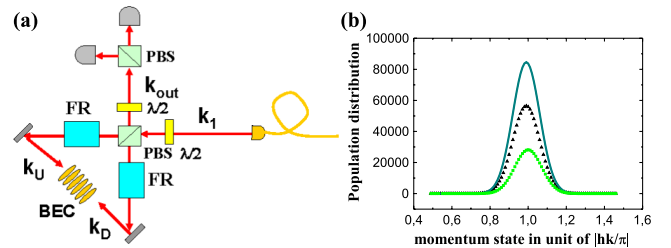


FIG. 3 (color online). (a) Interaction between the amplified field and the Bragg mBEC. The Faraday rotators (FR) allow the recombination of the reflected field on mode  $k_{\text{out}}$ . Indeed, the field with polarization  $\pi_H$  transmitted by the PBS on mode  $k_U$ , passing through the first FR at  $22.5^\circ$ , becomes  $\pi_+$  polarized. After the reflection by the Bragg mirror, its polarization is again rotated and becomes  $\pi_-$ : the field exits on mode  $k_{\text{out}}$ . A similar argumentation holds for the field polarized  $\pi_-$ . (b) Comparison between the expected populations of the first order momentum peaks (around 1% of total atoms) before and after the interaction. The dotted ( $\blacktriangle$ ) line represents the profile of the  $\pm 2\hbar k$  momentum state before interaction with the QI-OPA pulse; the continuous line and dotted ( $\blacksquare$ ) line represent the  $+2\hbar k$  and  $-2\hbar k$  momentum state profiles after interaction, respectively. Both heating and collisional effects have been neglected (see text).

direction  $\mathbf{k}_U$  ( $\mathbf{k}_D$ ). Two Faraday rotators inserted into the Sagnac-like interferometer allow the recombination of both the reflected fields  $\{|\phi^+\rangle_D, |\xi^-\rangle_U\}$  ( $\{|\xi^+\rangle_D, |\phi^-\rangle_U\}$ ) on the mode  $\mathbf{k}_{OUT}$  leading to the output state  $|\Phi^+\rangle_{OUT}|\Psi^U\rangle_{bec}$  ( $|\Phi^-\rangle_{OUT}|\Psi^D\rangle_{bec}$ ).

In the analysis above,  $|\Psi\rangle_{bec}$  represents the state of the interacting portion rather than of the overall BEC system. Indeed, the interaction with the QI-OPA pulse does not shift the BEC as a whole but only the atoms which get the momentum kick by the impinging photons. This mechanism of momentum transfer between light and atoms has been experimentally investigated in different works [26,27]. For a generic input photon macrostate  $|\Phi^\varphi\rangle$ , the resulting momentum exchange due to any elementary interaction will cause the spatial “displacement” of the mBEC depending on the phase  $\varphi$  encoded in the far apart Alice’s qubit [28]. The velocity acquired by the mBEC is  $\frac{N'}{N_{at}}v_r$ , where  $v_r$  is the condensate recoil velocity of rubidium (in this case, around 5 mm/s). This is visible during expansion where, due to the quantized nature of the momentum transfer, it appears as a transfer of atoms from the lower momentum state to a higher momentum state. Precisely, the normal momentum distribution of the mBEC is made of sharp peaks centered around zero. Because of the photon-atom collisions, a large number of atoms, for a total  $N'_\pm(\varphi)$ , will be transferred from the generic momentum state  $n2h/\lambda$  to the successive state  $(n \pm 1)2h/\lambda$ . The momentum state distribution then becomes asymmetric as reported in Fig. 3(b). There we show the result of a numerical simulation of the population transfer from the zero momentum to the first order momentum state, and we compare the population distributions after the interaction relative to the  $-2\hbar k$  and  $+2\hbar k$  momentum states. The lifetime of the macroscopic quantum superposition is limited by the decoherence between the original and the recoiled atomic wave packets. In Ref. [21], the decoherence rate for a matter-wave grating formed due to the CARL effect has been found experimentally to be  $6.4(9) \text{ ms}^{-1}$ . This should leave enough time to perform a measurement of nonlocal correlations. A preliminary experimental test on a sample mBEC with a classical light beam indeed showed a marked shift of the atomic momentum distribution due to light collision and a reflectivity in the range 0.5–0.9. As a further improvement to this scenario, in the experiment only the largest, most efficient optical pulses could be singled out by an ultrafast electro-optical switch placed at the output of the QI-OPA [29].

In conclusion, the entanglement structure of  $|\Sigma\rangle_{k_1, k_2}$  will imply the coherent displacement of the mBEC system, depending on the phase  $\varphi$  of the single photon measured by the far apart Alice’s apparatus. The correlation measurements could be carried out by detecting the reflected light in different polarization basis and by observing the momentum distribution of the atomic cloud. In addition, the reflection process effect could be repeated several times

by one or several external mirrors reflecting back the optical beams to the mBEC after the first interaction, leading an optical *cavity* structure, e.g., a Fabry-Perot interferometer, by which the BEC displacing effect could be enhanced by a “quality factor”  $Q \gg 1$ .

We acknowledge interesting discussions with C. Fort, L. Fallani, and M. Inguscio. F.D.M. also acknowledges early discussions with Markus Aspelmeyer leading to the basic idea of the present proposal. This work is supported by MIUR (N. PRIN 06), FP7 CHIMONO.

- 
- [1] W. Marshall *et al.*, Phys. Rev. Lett. **91**, 130401 (2003).
  - [2] H. Bohm *et al.*, Appl. Phys. Lett. **89**, 223101 (2006).
  - [3] S. Gigan *et al.*, Nature (London) **444**, 67 (2006).
  - [4] O. Arcizet *et al.*, Nature (London) **444**, 71 (2006).
  - [5] D. Kleckner *et al.*, Nature (London) **444**, 75 (2006).
  - [6] E. Schroedinger, Naturwissenschaften **23**, 823 (1935).
  - [7] *Bose-Einstein Condensation in Atomic Gases*, edited by M. Inguscio, C. Wieman, and S. Stringari (IOS Press, Tokyo, 1999).
  - [8] S. Inouye *et al.*, Science **285**, 571 (1999).
  - [9] M. Kozuma *et al.*, Science **286**, 2309 (1999); S. Inouye *et al.*, Nature (London) **402**, 641 (1999).
  - [10] L. Deng *et al.*, Nature (London) **398**, 218 (1999).
  - [11] F. De Martini, Phys. Lett. A **250**, 15 (1998); Phys. Rev. Lett. **81**, 2842 (1998).
  - [12] F. De Martini *et al.*, Phys. Rev. Lett. **95**, 240401 (2005).
  - [13] F. De Martini *et al.*, Phys. Rev. Lett. **100**, 253601 (2008).
  - [14] F. De Martini *et al.*, Phys. Rev. A **79**, 052305 (2009).
  - [15] E. Nagali *et al.*, Phys. Rev. A **76**, 042126 (2007).
  - [16] W. Schleich, *Quantum Optics in Phase Space* (Wiley, New York, 2001).
  - [17] F. Dalfovo *et al.*, Rev. Mod. Phys. **71**, 463 (1999).
  - [18] P. Pedri *et al.*, Phys. Rev. Lett. **87**, 220401 (2001).
  - [19] O. Morsch *et al.*, Rev. Mod. Phys. **78**, 179 (2006).
  - [20] R. Bonifacio *et al.*, Opt. Commun. **233**, 155 (2004).
  - [21] L. De Sarlo *et al.*, Eur. Phys. J. D **32**, 167 (2005).
  - [22] R. Bonifacio, Opt. Commun. **146**, 236 (1998); M. G. Moore *et al.*, Phys. Rev. A **60**, 1491 (1999).
  - [23] The last term in right-hand side of Eq. (1) represents the self-consistent optical wave grating while the first term in the right-hand side of Eq. (2) represents the self-consistent matter-wave grating. Equation (2) has been written in the “mean-field” limit, which models the propagation effects by a damping term where  $\kappa \approx c/2L$  and  $L$  is the BEC length.
  - [24] A more careful model should take into account a quasisinusoidal modulation of the refractive index due to the density distribution in the Thomas-Fermi approximation.
  - [25] M. Artoni *et al.*, Phys. Rev. Lett. **96**, 073905 (2006).
  - [26] G. Campbell *et al.*, Phys. Rev. Lett. **94**, 170403 (2005).
  - [27] M. F. Andersen *et al.*, Phys. Rev. Lett. **97**, 170406 (2006).
  - [28] Since the spatial displacement of the mBEC after the interaction with the QI-OPA pulse is too small to be directly detected, a standard “*expansion imaging*” technique will be adopted [7].
  - [29] N. Spagnolo *et al.*, Opt. Express **16**, 17 609 (2008).